Cellulose (2010) 17:387–398
DOI 10.1007/s10570-010-9396-8

DMA analysis and wood bonding of PVAc latex reinforced with cellulose nanofibrils

Francisco López-Suevos · Christian Eyholzer · Nico Bordeanu · Klaus Richter

Received: 4 September 2009 / Accepted: 2 January 2010 / Published online: 16 January 2010

Abstract Suspensions of commercial refined beech pulp (RBP) were further processed through mechanical disintegration (MD-RBP), chemical modification (CM-RBP) and through chemical modification followed by mechanical disintegration (CM-MD-RBP). Nanocomposites were prepared by compounding a poly(vinyl acetate) (PVAc) latex adhesive with increasing contents of the different types of nanofibrils, and the resulting nanocomposites were analyzed by dynamic mechanical analysis (DMA). Also, the suitability of using the CM-RBP fibrils to formulate PVAc adhesives for wood bonded assemblies with improved heat resistance was studied. The presence of cellulose nanofibrils had a strong influence on the viscoelastic properties of PVAc latex films. For all nanocomposites, increasing amounts of cellulose nanofibrils (treated or untreated) led to increasing reinforcing effects in the glassy state, but especially in the PVAc and PVOH glass transitions. This reinforcement primarily resulted from interactions between the cellulose fibrils network and the hydrophilic PVOH matrix that led to the complete disappearance of the PVOH glass transition (tan δ peak) for some fibril types and contents. At any given concentration in the PVOH transition, the CM-MD-RBP nanofibrils provided the highest reinforcement, followed by the MD-RBP, CM-RBP and the untreated RBP. Finally, the use of the CM-RBP fibrils to prepare PVAc reinforced adhesives for wood bonding was promising since, even though they generally performed worse in dry and wet conditions, the boards showed superior heat resistance (EN 14257) and passed the test for durability class D1.

Keywords Cellulose nanofibrils · Carboxymethylation · Mechanical disintegration · PVAc latex · Reinforcement · DMA · Wood bonding

F. López-Suevos (✉) · C. Eyholzer · N. Bordeanu · K. Richter
Empa, Swiss Federal Laboratories for Materials Testing and Research, Wood Laboratory Überlandstrasse 129, 8600 Dübendorf, Switzerland
e-mail: Fuco.lopezsuevos@gmail.com

F. López-Suevos
Centro de Innovación e Servizos Tecnolóxicos da Madeira de Galicia, CIS-Madeira, Avda. de Galicia, n°5, Parque Tecnolóxico de Galicia, 32901 San Cibrao das Viñas, Spain

C. Eyholzer
Division of Manufacturing and Design of Wood and Bionanocomposites, Luleå University of Technology (LTU), Luleå, Sweden

Introduction

Cellulose nanofibrils (CNF) derived from biomass resources are increasingly being used as reinforcing agents in the preparation of nanocomposites with polymer matrices due to their interesting properties, such as high strength and stiffness (Hubbe et al. 2008;

Yano and Nakahara 2004; Zadorecki and Michell 1989), transparency (Yano et al. 2005) or biodegradability (Couderc et al. 2009). Although CNF have been proved suitable to prepare nanocomposites with apolar matrices after chemical modification (e.g. silylation, TEMPO oxidation, acetylation or reactions with anhydrides) of the surface hydroxyl groups (Andresen et al. 2006; Araki et al. 2001; Goussé et al. 2004; Lasseuguette 2008; Saito et al. 2006; Sassi and Chanzy 1995; Stenstad et al. 2008), the hydrophilic nature of CNF makes them especially attractive for polar matrices such as PVOH (Zimmermann et al. 2005; Roohani et al. 2008; Lu et al. 2008), hydroxypropyl cellulose (Zimmermann et al. 2005), acrylic and phenol–formaldehyde resins (Iwamoto et al. 2007; Nakagaito and Yano 2004, 2005, 2008), or poly(styrene-co-butyl acrylate) (Samir et al. 2004; Dalmas et al. 2007) and PVAc (De Rodriguez et al. 2006) latexes. However, the main drawback of using the hydrophilic CNF is that they have to be stored as aqueous suspensions (10–30 wt%) since irreversible agglomeration of the fibrils through hydrogen bonding will occur during drying, i.e. hornification (Young 1994; Hult et al. 2001). Fortunately, partial carboxymethylation of the CNF is well-known to prevent hornification (Bordeanu et al. 2008; Cantiani et al. 2001a, b, c; Cash et al. 2000; Eyholzer et al. 2009; Dinand et al. 1996; Excoffier et al. 1999; Herrick 1984; Laivins and Scallan 1993; Lindström and Carlsson 1982), and consequently, carboxymethylated CNF (highly hydrophilic) can be obtained in powder form that is water-redispersible. Finally, in addition to adequate fibril/matrix chemical affinity, attainable reinforcement levels are closely related to the degree of mechanical disintegration of the fibrils. Therefore, the mechanical properties of nanocomposites can be modified by properly processing and refining the CNF (Zimmermann et al. 2004).

The mechanical properties of nanocomposites can be efficiently evaluated by dynamic mechanical thermal analysis (DMA) as a function of time/frequency and temperature. Moreover, DMA is especially suited to identify fibril/matrix interactions or changes in the viscoelastic properties of nanocomposites in the glassy, glass transition and rubbery plateau regions. For instance, Lu et al. (2008) showed that increasing amounts of microfibrillated cellulose (derived from kraft pulp) to a PVOH matrix led to a significant increase of the storage modulus in the glassy region and especially in the rubbery plateau. Kvien and Oksman (2007) reported a significant difference in storage modulus in the glassy region of a PVOH matrix when using cellulose nanowhiskers (CNW) oriented in parallel or transverse directions. Dalmas et al. (2007) showed that cellulose nanofibrils obtained from sugar beet pulp provided a large mechanical reinforcement to an amorphous poly(styrene-co-butyl acrylate) matrix in the rubbery plateau region. This effect was explained by the formation of a rigid nanofibril network through hydrogen bonding, which was governed by a percolation mechanism (Azizi Samir et al. 2005). Alemdar and Sain (2008) showed the reinforcing effect of wheat straw cellulose nanofibers in a starch-based thermoplastic polymer (TPS). Interestingly, the presence of the nanofibers remarkably shifted the neat TPS glass transition temperature (Tg) 30–40 °C, which was attributed to interfacial TPS/nanofibers interactions. Similarly, Kristo and Biliaderis (2007) attributed the significant increase in the sorbitol-plasticized pullulan Tg with increasing amounts of starch nanocrystals to strong filler/filler and filler/polymer interactions. In summary, these studies demonstrate the potential of the DMA technique to identify fibril/polymer interactions and to evaluate reinforcement effects in the viscoelastic response of cellulose nanocomposites.

In the present work, the aqueous RBP suspensions were further processed through chemical modification (CM-RBP), mechanical disintegration (MD-RBP) and through chemical modification followed by mechanical disintegration (CM-MD-RBP). Nanocomposites were prepared by mixing a commercial PVAc latex with different concentrations of the untreated or the processed RBP fibrils. The resulting nanocomposites were analyzed by DMA to investigate the influence of the different types of cellulose nanofibrils on the PVAc viscoelastic properties and to identify possible fibril/PVAc interactions. Finally, the suitability of the CM-RBP fibrils to prepare PVAc adhesives intended for wood bonded assemblies with enhanced heat resistance was evaluated.

Materials and methods

Materials

The refined, bleached beech pulp (RBP) was provided by J. Rettenmaier & Söhne GmbH, Rosenberg,

Germany (Arbocel B1011, 10 wt% aqueous suspension. The chloroacetic acid (sodium salt, purity ≥ 98%) and the glacial acetic acid (purity ≥ 99.8%) were purchased from Merck (Darmstadt, Germany), and the sodium hydroxide (NaOH, purity ≥ 98%) from Fluka (Buchs, Switzerland).

The commercial PVAc latex used was VN 1693 (Collano AG, Switzerland) with a solids content of 49.5 ± 0.1%. This system is an aqueous suspension of PVAc particles stabilized by PVOH and it does not contain cross-linking agents. This is a thermoplastic wood adhesive for non-structural applications classified as suitable for durability class D3 (EN 204:2001) by the provider. Briefly, durability class 3 implies that the bonded member can be used in interior with frequent short-term exposure to running or condensed water and/or to heavy exposure to high humidity. Also, it can be used in exterior not exposed to weather.

Mechanical disintegration

About 1.40 kg of the RBP aqueous suspension (ca. 10 wt%) were initially mixed with 8 L of water and stirred with a stainless steel agitator for 30 min at 20 °C in a 10 L reactor. The diluted RBP suspension (ca.1.5 wt%) was then processed with an inline disperser (Megatron MT 3000, Kinematica AG, Switzerland) at 20,000 rpm for 60 min. This pretreatment facilitated the breaking down of the RBP fibrous material into smaller parts (cellulose fibril bundles) providing a more homogeneous suspension. Then, 6 L of the pretreated RBP suspension were subjected to high-shear disintegration in a Microfluidizer type M-110Y (Microfluidics Corporation, USA). A stable cellulose nanofibril suspension (MD-RBP) was obtained after 6 passes through the $H230Z_{400\ \mu m}$ and $F20Y_{75\ \mu m}$ interaction chambers of the microfluidizer. The estimated processing pressure inside the F20Y chamber was 125 MPa.

Chemical modification

About 2.54 kg of the 10 wt% RBP aqueous suspension were transferred to a 10 L reactor equipped with the inline disperser and a mechanical stirrer, and then 7.46 kg of a 5/3 v/v isopropanol/ethanol mixture were added. The resulting mixture was processed with the inline disperser at 15,000 rpm for 30 min at 20 °C followed by slow addition of 189.50 g of a 21 wt% sodium hydroxide aqueous solution under continuous stirring to activate the cellulose. Then, 115.02 g of chloroacetic acid (sodium salt) were added to the activated suspension and the temperature was increased to 60 °C. The reaction mixture was again processed with the inline disperser at 20,000 rpm for 2 h before cooling it down to 20 °C to stop the reaction. The resulting suspension was neutralized with acetic acid and centrifuged at 15,000 rpm for 90 min. The supernatant was discarded and the precipitate containing the carboxymethylated cellulose fibrils was washed first with distilled water three times to remove any water-soluble by-product and second with a 5/3 v/v isopropanol/ethanol mixture prior to drying overnight in the oven at 65 °C. The resulting powdered CM-RBP fibrils are easily re-dispersable in water forming a stable gel. The degree of substitution (DS) of the CM-RBP was evaluated by conductometric titration according to a modified method from Eyler et al. (1947) and described in a previous study (Eyholzer et al. 2009). A DS of 0.156 ± 0.028 was obtained from three independent evaluations, which amounts to 5.2% of the hydroxyl groups present in the cellulose fibrils being replaced by carboxyl groups. As a reference, when the DS of the CM-RBP is greater than 0.25 the cellulose fibrils become soluble in water (Eyholzer et al. 2009).

Finally, the CM-MD-RBP fibrils were prepared by initially re-dispersing 69.2 g of the dry CM-RBP in 2.69 kg of water (ca. 2.5% by weight) with a high-shear blender (Ultra-Turrax, IKA, Germany). The resulting suspension was then transferred to the 10 L reactor and the mechanical disintegration treatment was conducted as previously described.

Preparation of nanocomposites

Composites were prepared by mixing the PVAc latex with the RBP, MD-RBP, CM-RBP or CM-MD-RBP fibrils at different concentrations, i.e. 5, 10, 20 and 30 wt% (g of dry fibrils in 100 g of total dry material). The PVAc-fibrils mixtures were blended with the Ultra-Turrax and degassed under vacuum before casting the films onto silicon molds. The films were dried under ambient conditions for 2 days and then cut with a twin-bladed cutter to obtain 45 (length) × 10 (width) × 0.6–0.7 (thickness) mm samples. Prior to

DMA analysis, all samples were dried by storage over silica gel under vacuum for at least 3 days.

Field emission scanning electron microscopy

The surface of the PVAc nanocomposites (previously dried as described for the DMA samples) with 10 and 30 wt% of the CM-MD-RBP fibrils were evaluated on a Jeol 6300F FE-SEM (Jeol Ltd., Japan) instrument. For the preparation of the FE-SEM samples, glimmer plates bonded to the sample's holder with a conducting carbon paste were employed. The samples were placed on the glimmer plates, and then coated with a platinum layer of 9 nm (*BAL-TEC MED 020* modular high vacuum coating system, BAL-TEC AG, Principality of Liechtenstein). The FE-SEM experiments were conducted at an accelerating voltage of 5 kV.

DMA experiments

A GABO-Eplexor DMA 800 (GABO qualimeter Testanlagen GmbH, Germany) in tension mode was used to study the viscoelastic properties of the resulting dried PVAc nanocomposites. All samples were initially conditioned at 0 °C for 5 min in the DMA, and then dynamic heating scans were performed from 0 to 150 °C at 2 °C/min and 10 Hz. The contact force, the static load strain and the dynamic load strain used in these experiments were 0.1 N, 0.3 and 0.03%, respectively. Three analyses were obtained for each sample.

Assessment of adhesive performance

Three adhesive formulations, namely, the neat PVAc and the PVAc with 1 and 3 wt% of the CM-RBP were selected to prepare three bonded panels of $1000 \times 135 \times 10$ mm^3 using beech wood ($10.8 \pm 0.5\%$ moisture content, $n = 10$). The preparation details of the bonded assemblies with these three adhesives are shown in Table 1. Each panel was cut into individual test specimens of $150 \times 20 \times 10$ mm according to EN 205:2003. The resulting 30 lap joint test pieces per board were randomly distributed into three treatment groups (Table 2): (1) 10 specimens were conditioned at (20 ± 2) °C and $(65 \pm 5)\%$ relative humidity for 7 days (Standard atmosphere or durability class D1, EN 204:2001), (2) 10 specimens were conditioned in the above standard atmosphere followed by 4 days in water at (20 ± 5) °C (Durability class D3, EN 204:2001) and (3) 10 specimens were conditioned in the described standard atmosphere and then each test piece was heated for 1 h in a preheated fan oven at 80 °C (WATT ′91 test) according to EN 14257:2006. Immediately after each treatment, the specimens were tested in a Universal Testing Machine (Zwick 1474, Zwick GmbH & Co. KG, Germany) to evaluate the tensile shear strength parallel to the grain.

Table 1 Preparation of Beech bonded assemblies with three PVAc formulations

Boards	1	2	3
Adhesive	PVAc	PVAc with 1% CM-RBP	PVAc with 3% CM-RBP
Solids content (%)[a,c]	49.5 ± 0.1	46.0 ± 0.2	40.8 ± 0.2
Apparent viscosity[b,c] (Pa.s)	9.55 ± 0.07	3.16 ± 0.02	3.83 ± 0.01
Spreading rate[d] (g/m^2)		185[f]	
Open time (min)[e]		5[f]	
Pressure (N/mm^2)		0.3[f]	
Press time (h)		2[f]	
Press temperature (° C)		20–21[f]	

[a] Determined according to ASTM D 1489-87

[b] Measurement at 14.38 s^{-1} and 20 °C using a cone (40 mm, 1.59°)/plate in a Physica MCR 300 rheometer

[c] Average value for three samples with standard deviation

[d] Amount and application is on each bonding surface

[e] Time elapsing from adhesive application to assembly of the lamellas

[f] The same value was used for the three adhesive formulations

Table 2 Conditioning treatments for the lap joint test pieces and minimum required tensile shear strength values

Treatment	Duration and condition	Shear strength (N/mm^2)	European standard
Durability class D1	7 days in standard atmosphere[a]	≥10	EN 204 and 205
Durability class D3	7 days in standard atmosphere[a]	≥2	EN 204 and 205
	4 days in water at (20 ± 5) °C		
WATT ′91	7 days in standard atmosphere[a]	Not specified[b]	EN 14257
	(60 ± 2) min at (80 ± 2) °C		

[a] (20 ± 2) °C and (65 ± 5)% relative humidity

[b] In general, there is not specific requirement; only when the adhesive is intended for window sections a shear strength higher than 7 N/mm^2 is required

The rate of separation of the jaws was 50 mm/min for all samples. Specifically for the WATT ′91 test, the time between removal of the test piece from the oven and the start of the test has to be 9 ± 1 s.

Additionally, the steady-state flow properties of these liquid PVAc adhesives were measured in order to find out the influence of the CM-RBP fibrils on the PVAc rheological behaviour. These experiments were conducted in a Physica MCR 300 rheometer at 20 °C using a cone (40 mm, 1.59°)/plate from 100 to 1 s^{-1} of shear rate. The resulting flow curves were fitted to the Power law equation ($\tau_{zx} = k\,(dVz/dx)^n$), where τ_{zx} is the shear stress (Pa), (dVz/dx) is the shear rate (s^{-1}), k is the consistency index ($Pa.s^n$) and n is the power law index (Fig. 1). The fit was conducted collectively on three data sets from the respective sample types and the goodness of fit (R^2) was always higher than 0.99.

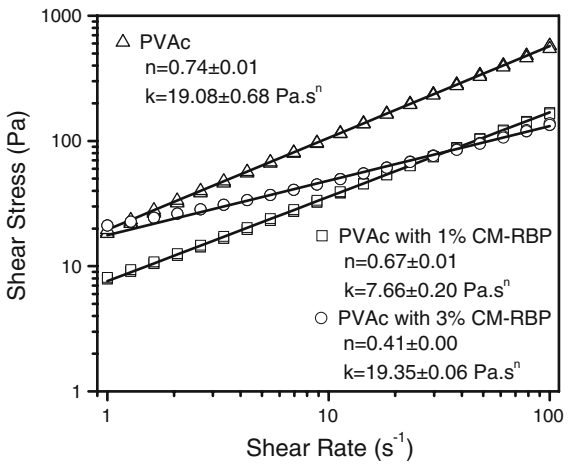

Fig. 1 Flow curves of the three liquid PVAc adhesives fitted to the Power law equation (*solid lines*) showing the consistency (k) and the power law (n) indexes. The fit was conducted collectively on three data sets from the respective sample types and the goodness of fit (R^2) was always higher than 0.99

Statistical analysis

One-way analysis of variance (ANOVA) was performed on the shear strength data for each treatment, with the adhesive type as independent variable. Tukey multiple comparison tests were conducted if a significant difference ($p \leq 0.05$) existed. Version 2.03 of the Windows SigmaStat software was used to conduct this statistical analysis.

Results and discussion

Figures 2 and 3 show the evolution of the storage modulus (top graphs) and tan δ (bottom graphs) with temperature for the PVAc nanocomposites prepared with the the RBP and CM-RBP (Fig. 2), and MD-RBP and CM-MD-RBP (Fig. 3) fibrils at different concentrations (i.e. 0, 5, 10, 20 and 30 wt%). All graphs show the same temperature, storage modulus and tan δ scales in order to facilitate comparisons between nanocomposites. Also, inset graphs of the storage modulus response in the low temperature region are provided to help visualize differences. The reproducibility of the viscoelastic response was very good, as demonstrated by the nearly perfect overlap of three repeat curves for each sample type. Spanning from low to high temperatures, three different regions can be identified in the neat PVAc films (open circle symbols): the glassy state (approx. below 25 °C), the PVAc glass transition (25–65 °C) (López-Suevos and Frazier 2005; Backman and Lindberg 2004) with a tan δ peak near 45 °C, and the very broad PVOH glass transition (65–150 °C) (López-Suevos and

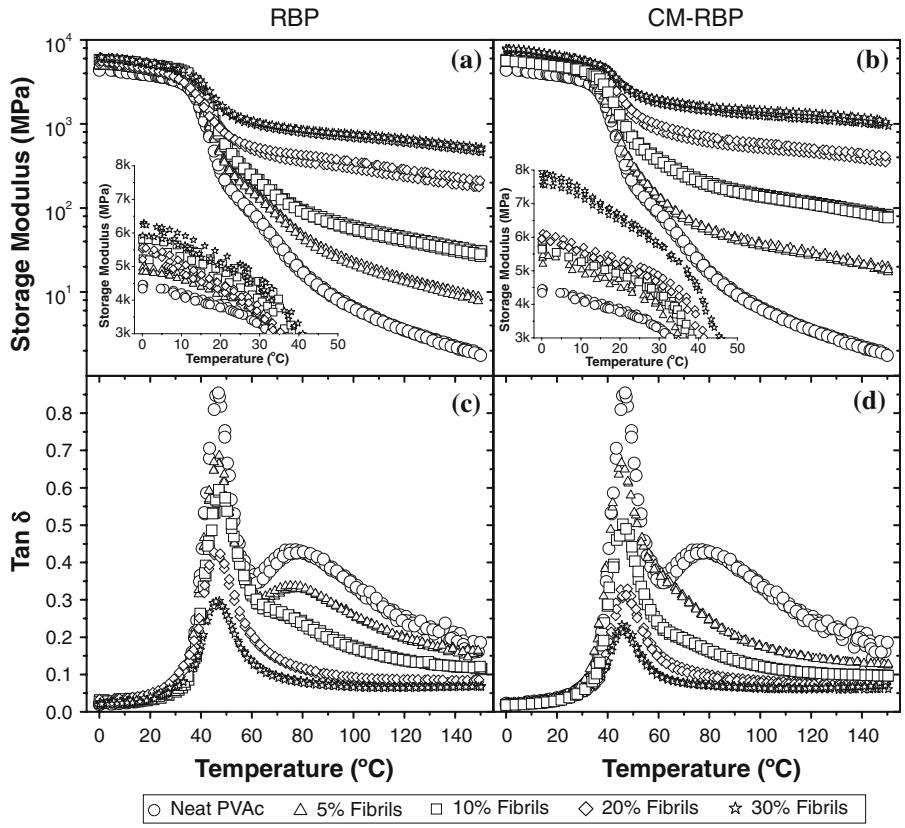

Fig. 2 Dynamic heating scans showing the storage modulus (*top graphs*) and tan δ (*bottom graphs*) for PVAc composites prepared with the RBP and CM-RBP cellulose fibrils at 0, 5, 10, 20 and 30 wt%. Three repetitions at each concentration are shown. *Insets* show expanded plot of the storage moduli in the low temperature region (glassy region)

Frazier 2006) with a tan δ peak around 80 °C. As the temperature increased through these two glass transitions the neat films dramatically softened, as showed by the almost four decade reduction in storage modulus.

First of all, it should be highlighted that the presence of the cellulose nanofibrils had a remarkable effect on the viscoelastic properties of the resulting nanocomposites, regardless of the fibril type (treated or untreated) and content. This was demonstrated by an increase in their storage modulus in the whole temperature range and a decrease in the tan δ intensity above the PVAc glassy state (Figs. 2, 3). We defined a reinforcement factor, RF, calculated by dividing the storage modulus for each composite by the storage modulus of the neat PVAc at the same temperature, i.e. the RF is the number of times the storage modulus was increased by the presence of the fibrils (Table 3). When considering the glassy region (see inset graphs of Figs. 2, 3 or Table 3, column for 0 °C), the storage modulus moderately increased with increasing loadings of each type of cellulose nanofibrils (RF values ranging from 1.11 to 1.39 for the RBP, 1.21 to 1.76 for the CM-RBP, 1.12 to 1.57 for the MD-RBP and 1.15 to 1.64 for the CM-MD-RBP nanocomposites). Interestingly, when the different fibrils were compared at the same concentrations, the reinforcement provided by the untreated RBP fibrils was quite similar to that of the treated fibrils (CM-RBP, MD-RBP and CM-MD-RBP) at 5 and 10 wt% but markedly smaller at 20 and 30 wt% (Table 3, column for 0 °C).

In the PVAc glass transition, on the one hand, the presence of cellulose fibrils did not significantly alter the PVAc glass transition temperature (±2 °C from tan δ peak) suggesting, according to similar studies (Backman and Lindberg 2004), a weak interaction between the bulk PVAc particles and the fibrils. Indeed, since PVAc is hydrophobic, it seems very unlikely that the fibrils would penetrate into a neat

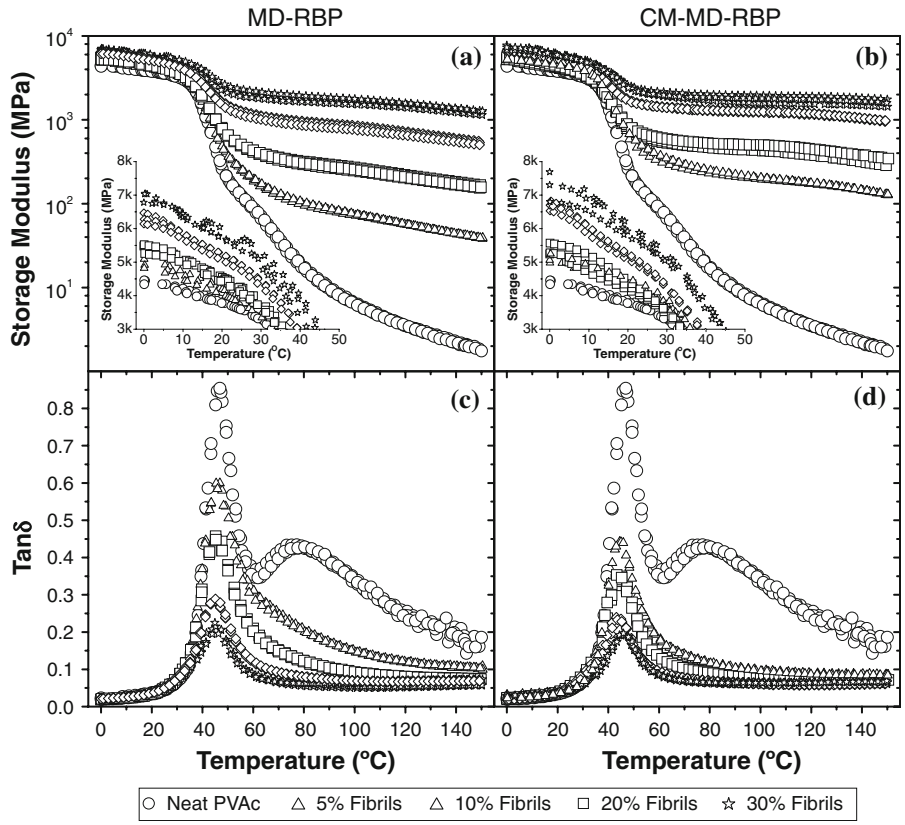

Fig. 3 Dynamic heating scans showing the storage modulus (*top graphs*) and tan δ (*bottom graphs*) for PVAc composites prepared with the MD-RBP and CM-MD-RBP cellulose nanofibrils at 0, 5, 10, 20 and 30 wt%. Three repetitions at each concentration are shown. *Insets* show expanded plot of the storage moduli in the low temperature region (glassy region)

PVAc region. On the other hand, the storage modulus in the PVAc glass transition significantly increased up to nearly 1.5 decades and the damping intensity (tan δ peak) decreased from 0.85 to 0.19, depending on the fibril type and concentration (maximum storage modulus and minimum tan δ intensity were obtained when using 30 wt% of the CM-MD-RBP).

Even more significant was the effect of the fibrils in the PVOH glass transition, which led to increases in the storage modulus of up to three decades with respect to the neat PVAc films (Figs. 2, 3). For each type of fibril, the RF values dramatically increased, especially at 150 °C, with increasing fibril contents. For example, the RF varied (at 150 °C) from 6.6 to 494 for the RBP, 17 to 1001 for the CM-RBP, 37 to 1208 for the MD-RBP, and 126 to 1588 for the CM-MD-RBP nanocomposites. More interestingly, the presence of the fibrils also led to the gradual disappearance of the tan δ peak with increasing fibril contents (Figs. 2, 3). These effects are associated with the segmental motions of the PVOH chains being increasingly restricted by the presence of the nanofibrils network and their strong interaction with the highly hydrophilic PVOH. Also, because of chain transfer reactions during polymerization of the PVAc, it is very likely that PVOH is covalently bonding the particle surfaces acting much like a capsular barrier. Because of this, the reinforcement observed in the PVAc glass transition might also be attributed to these strong PVOH/fibril interactions and possibly to fibril/fibril interactions (within the PVOH matrix) at the particle boundaries. Since PVOH is dispersed around the PVAc particles, it is clear that effects at the PVOH-rich boundaries will have an impact on the PVAc bulk particles. Supporting this mechanism, SEM images from nanocomposites with 10 and 30 wt% of CM-MD-RBP (Fig. 4) showed that cellulose nanofibrils mostly form a compact network covering the surface of the PVAc particles and the interparticle regions. They also showed some isolated cellulose

Table 3 Storage modulus and reinforcement provided by the differently treated cellulose fibrils (chemical, mechanical or both) at different concentrations at 0, 80 and 150 °C

PVAc nanocomposite	0 °C		80 °C		150 °C	
	Storage modulus (MPa)	Reinforcement factor[a]	Storage modulus (MPa)	Reinforcement factor[a]	Storage modulus (MPa)	Reinforcement factor[a]
Neat PVAc	4417 (67)	1	17 (0)	1	1.8 (0.1)	1
5% RBP	4900 (60)	1.11 (0.02)	44 (1)	2.6 (0.1)	8.4 (0.6)	4.6 (0.4)
5% CM-RBP	5347 (133)	1.21 (0.04)	56 (2)	3.3 (0.1)	19 (1)	10 (1)
5% MD-RBP	4940 (138)	1.12 (0.04)	99 (5)	5.9 (0.3)	39 (1)	21 (1)
5% CM-MD-RBP	5097 (139)	1.15 (0.04)	242 (8)	14 (1)	128 (1)	70 (3)
10% RBP	5543 (293)	1.26 (0.07)	93 (2)	5.5 (0.2)	29 (2)	16 (1)
10% CM-RBP	5717 (100)	1.29 (0.03)	189 (9)	11 (1)	74 (3)	40 (2)
10% MD-RBP	5420 (140)	1.23 (0.04)	305 (13)	18 (1)	152 (6)	83 (5)
10% CM-MD-RBP	5363 (180)	1.21 (0.04)	490 (32)	29 (2)	326 (29)	178 (17)
20% RBP	5430 (193)	1.23 (0.05)	389 (38)	23 (2)	194 (17)	106 (10)
20% CM-RBP	6003 (92)	1.36 (0.03)	653 (53)	39 (3)	376 (27)	205 (17)
20% MD-RBP	6297 (166)	1.43 (0.04)	911 (54)	54 (3)	519 (24)	283 (18)
20% CM-MD-RBP	6683 (146)	1.51 (0.04)	1302 (26)	78 (2)	983 (12)	536 (23)
30% RBP	6150 (210)	1.39 (0.05)	829 (44)	49 (3)	496 (33)	270 (21)
30% CM-RBP	7760 (185)	1.76 (0.05)	1532 (115)	91 (7)	1003 (57)	547 (39)
30% MD-RBP	6953 (150)	1.57 (0.04)	1775 (144)	106 (9)	1210 (68)	660 (46)
30% CM-MD-RBP	7263 (446)	1.64 (0.10)	1850 (152)	110 (9)	1590 (160)	867 (95)

All values are the average for three samples with standard deviation (in parentheses)

[a] The reinforcement factor (RF) was calculated by dividing the storage modulus for each composite by the storage modulus of the neat PVAc, i.e. the RF is the number of times the storage modulus was increased by the presence of the fibrils

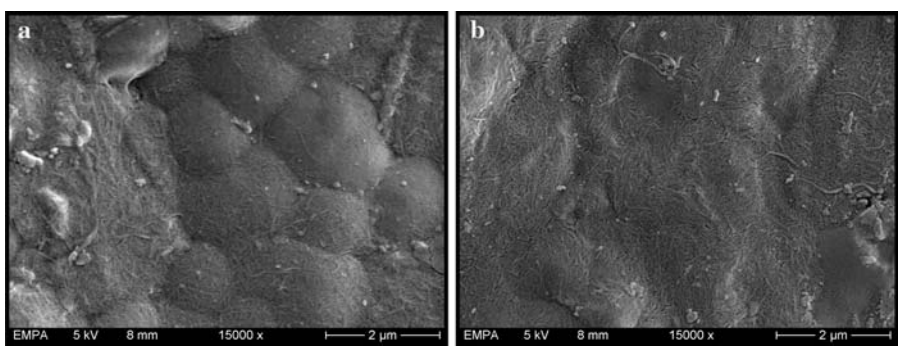

Fig. 4 FE-SEM surfaces of PVAc nanocomposites with 10(**a**) and 30 (**b**) wt% of the CM-MD-RBP cellulose fibrils

fibril aggregates that were not completely refined during the chemical and mechanical treatments.

When considering all nanocomposites at any given fibril content, those prepared with the CM-MD-RBP nanofibrils clearly showed the highest RF values at 80 and 150 °C followed by the MD-RBP, CM-RBP and the untreated RBP fibrils. Differences between the treatments were maximum at lower contents and decreased when the fibril contents increased. These differences between the treatments might be

explained because mechanical disintegration of the RBP (MD-RBP) breaks down the RBP fibrous material into thinner parts providing cellulose nanofibrils with higher aspect ratio, and consequently, with higher reinforcing potential (Chakraborty et al. 2006). On the other hand, carboxymethylation of the RBP nanofibers (CM-RBP) increases the degree of swelling of the fibers and opens up the fiber structure (Walecka 1956), facilitating not only fiber/fiber and fiber/matrix interactions but also further microfibrillation (CM-MD-RBP) (Wågberg et al. 2008). In fact, a synergistic effect between the treatments was found at 5 and 10 wt% and 5, 10 and 20 wt% fibril loadings at 80 and 150 °C, respectively. This is shown by a synergy ratio, defined as the RF provided by the cellulose nanofibrils that were first chemically modified and subsequently mechanically disintegrated (CM-MD-RBP) divided by the sum of the individual RFs due to the fibrils that were chemically (CM-RBP) and the fibrils that were mechanically modified (MD-RBP), greater than 1 for these compositions (Table 4). As expected, this synergistic effect was more significant for nanocomposites prepared with the lowest fibril content (5 wt%) with ratios around 1.6 (80 °C) and 2.2 (150 °C), suggesting that the CM-MD-RBP nanofibrils form the most effective percolating network within the PVOH matrix. As the fibril content increased, the synergistic effect was progressively reduced and it vanished for nanocomposites with 20 and 30 wt% at 80 °C and for nanocomposites with 30 wt% at 150 °C (ratio < 1). Consequently, from an economical point of view, the extra cost in treating and obtaining the CM-MD-RBP fibrils might limit their use to low concentrations, whereas at high concentrations (e.g. 30 wt%) the MD-RBP fibrils (RF of 1208 at 150 °C), the CM-RBP (RF of 1001 at 150 °C) or even the untreated RBP (RF of 494 at 150 °C) might be a better choice than the CM-MD-RBP (RF of 1588 at 150 °C).

Table 4 Synergistic effects between treatments at 80 and 150 °C

Fibril content (%)	Synergy ratio[a]	
	80 °C	150 °C
5	1.56 (0.07)	2.23 (0.06)
10	1.01 (0.07)	1.44 (0.13)
20	0.83 (0.04)	1.10 (0.05)
30	0.56 (0.06)	0.72 (0.08)

All values are the average for three samples with standard deviation (in parentheses)

[a] The synergy ratio is defined as the ratio of the reinforcement factor (RF) due to the fibrils that were chemically modified followed by mechanical disintegration (CM-MD-RBP, treatments acting together) divided by the sum of the individual RFs due to the fibrils that were chemically (CM-RBP) and the fibrils that were mechanically modified (MD-RBP) at the same concentration. A ratio higher than 1 implies a synergistic effect

Considering the outstanding reinforcing potential provided by the studied cellulose fibrils to the PVAc latex adhesive in the high temperature region, a preliminary study on their suitability to prepare wood adhesives to manufacture beech bonded assemblies with higher heat resistance was conducted. Therefore, three adhesive formulations, namely, the neat PVAc and the PVAc with 1 and 3 wt% of the CM-RBP were employed to prepare boards as previously described (Table 1). The CM-RBP fibrils were chosen for this study, regardless of the lower reinforcing potential respect to the MD-RBP and CM-MD-RBP (both obtained as aqueous suspensions), because they were obtained in powder form (but easily redispersible in water). Therefore, the CM-RBP fibrils are not only more stable (especially against bacterial decomposition) allowing significant savings in storage and, consequently, in shipping, but also they facilitate the preparation of wood adhesives with a tailored solids content and a better control of the viscosity prior to wood bonding. In particular, the addition of the CM-RBP fibrils to the neat PVAc latex led to a more pseudoplastic behaviour of the resulting adhesives as the power law index (n) decreased from 0.74 to 0.41 (Fig. 1). This behavior is of great interest because, as the adhesive is subjected to stress during its application, its apparent viscosity will decrease, resulting in better flow, and consequently enhancing the spreading of the adhesive over the wood surface.

Table 5 shows the average shear strength with standard deviation for the three boards after the conditioning treatments (Table 2). As it can be observed, all boards easily met the requirement for durability class D1 (dry shear strength > 10 N/mm^2). However, one-way ANOVA showed that the addition of fibrils had a detrimental effect on the shear strength of the boards ($p < 0.05$) when tested in dry conditions, and both boards prepared with 1 and 3% of CM-RBP fibrils showed significantly lower shear strengths than the neat PVAc. When the requirement for

Table 5 Average shear strength values with standard deviation for boards 1–3 after the conditioning treatments (see Table 2 for details)

Board	Adhesive	Shear strength (N/mm^2)		
		Durability class D1[1]	Durability class D3[1]	WATT 91[1]
1	Neat PVAc	19.4 ± 2.8^{a}	1.7 ± 0.3^{a}	4.6 ± 0.6^{a}
2	PVAc-1% CM-RBP	14.7 ± 0.6^{b}	1.4 ± 0.2^{b}	5.1 ± 0.7^{a}
3	PVAc-3% CM-RBP	14.8 ± 1.1^{b}	$1.5 \pm 0.2^{a,b}$	5.9 ± 0.4^{b}

One-way analysis of variance was performed on the shear strength data for each treatment

[1] For each treatment, same letter indicates that the shear strength data is not significantly different

durability class D3 (wet shear strength > 2 N/mm^2) was tested, surprisingly, none of the boards prepared passed the test. This was unexpected, since the commercial neat PVAc used in this study was classified as suitable for durability class D3 by the provider. Again, one-way ANOVA showed that the addition of fibrils had an adverse effect on the properties of the boards ($p < 0.05$). However, in this case, the average shear strength value for the board with 3 wt% of CM-RBP fibrils was not significantly different than that of the neat PVAc adhesive. Finally, when tested in the WATT 91 test (briefly, lap joint specimens tested after 1 h at 80 °C), addition of the fibrils also had a significant effect (one-way ANOVA, $p < 0.05$) but in this case, positive, since the board reinforced with 3 wt% of fibrils showed a significantly higher shear strength value than the control sample. This indicates a significant increase in heat resistance when using the PVAc adhesive reinforced with 3 wt% fibrils and it is in agreement with the reinforcing effect observed in Table 3 (DMA data) at 80 °C for all nanocomposites containing the CM-RBP fibrils. The observed decrease in adhesion (durability class D1) might be associated to the reduction in apparent viscosity induced by the fibrils (the neat PVAc apparent viscosity was approx. three times higher than those for the adhesives containing the fibrils). This, while improving spreadability, might also result in an increased penetration of the fibril-containing adhesives into the wood which in turn could lead to a weaker glue line. In addition, the presence of the cellulose nanofibrils might also perturb the film forming process of PVAc negatively affecting adhesion. On the other hand, the fact that carboxymethylated cellulose fibrils are quite hydrophilic and consequently, more accessible to water might explain the reduction in durability. Finally, in agreement with the DMA data, the presence of the fibrils is stiffening the glue line which while not contributing to improve adhesion at room temperature, becomes essential when tested at 80 °C. Collectively, these results indicated that the addition of the carboxymethylated fibrils (CM-RBP) to a PVAc latex effectively enhanced the heat resistance of the glue line of beech bonded assemblies but generally reduced its performance under dry (durability class D1) and wet conditions (durability class D3). Further studies will be conducted to optimize the main parameters involved in the PVAc preparation (e.g. solids content, viscosity, cellulose fibril content, other type of cellulose fibrils, other type of PVAc latex, etc.) in an attempt to prepare adhesive formulations that will also fulfill the durability class D3 and WATT 91 requirements.

Conclusions

The untreated and processed cellulose nanofibrils used in this work had a remarkable influence on the viscoelastic properties of PVAc latex films as demonstrated by significant increases in storage modulus in the whole temperature range and by significant decreases in tan δ above the glassy state. This was mainly attributed to a strong interaction between the cellulose nanofibrils network and the highly hydrophilic PVOH matrix that dramatically restricted segmental motions of the PVOH chains. Among the different cellulose nanofibrils at any given concentration in the high temperature region, those that were carboxymethylated and subsequently mechanically disintegrated provided the largest reinforcement followed by those that were only mechanically disintegrated, those that were only carboxymethylated, and the untreated ones. However, the higher technical and

energetic operating expenses necessary to produce the CM-MD-RBP fibrils might only be justifiable when they are used at very low contents (5 wt%), where the difference in reinforcement respect to the other types of fibrils is maximum. Otherwise, the simple mechanical treatment seems a better choice since the resulting fibrils not only provide a large reinforcement at a smaller processing cost but also they are less hydrophilic than the carboxymethylated fibrils and therefore less accessible to water. This proved important when the CM-RBP fibrils were used to prepare adhesives, since boards prepared with this type of fibrils clearly passed the test for durability class D1 and showed significantly enhanced heat resistance (EN 14257), but failed the test for durability class D3.

Collectively, these findings are encouraging to conduct a more thorough study with the other types of fibrils, especially the MD-RBP, and PVAc latexes so that the durability class 3 and specific heat resistance requirements (e.g. for windows sections the shear strength > 7 N/mm^2) are met.

Acknowledgments The authors would like to thank Mr. Daniel Heer, Mr. Walter Risi and Mr. Michael Strässle (Wood Lab, Empa) for their technical assistance in the manufacture, ageing and testing treatments, respectively, of the bonded assemblies.

References

Alemdar A, Sain M (2008) Biocomposites from wheat straw nanofibers: morphology, thermal and mechanical properties. Compos Sci Technol 68(2):557–565

Andresen M, Johansson LS, Tanem BS, Stenius P (2006) Properties and characterization of hydrophobized microfibrillated cellulose. Cellulose 13:665–677

Araki J, Wada M, Kuga S (2001) Steric stabilization of a cellulose microcrystal suspension by poly(ethylene glycol) grafting. Langmuir 17:21–27

Azizi Samir MAS, Alloin F, Dufresne A (2005) Review of recent research into cellulosic whiskers, their properties and their application in nanocomposite field. Biomacromolecules 6:612–626

Backman AC, Lindberg KAH (2004) Interaction between wood and polyvinyl acetate glue studied with dynamic mechanical analysis and scanning electron microscopy. J Appl Polym Sci 91:3009–3015

Bordeanu N, Eyholzer C, Zimmermann T (2008) Cellulose nanostructures with tailored functionalities. Pending patent

Cantiani R, Guerin G, Senechal A, Vincent I, Benchimol J (2001a) Supplementation of cellulose nanofibrils with carboxycellulose with low degree of substitution. US patent 6231657

Cantiani R, Guerin G, Senechal A, Vincent I, Benchimol J (2001b) Additivation of essentially amorphous cellulose nanofibrils with carboxyl cellulose with a high degree of substitution. US patent 6224663

Cantiani R, Guerin G, Senechal A, Vincent I, Benchimol J (2001c) Supplementation of essentially amorphous cellulose nanofibrils with carboxycellulose which has a high degree of substitution. US patent 6306207

Cash MJ, Chan AN, Conner HT, Cowan PJ, Gelman RA, Lusvardi KM, Thompson SA, Tise FP (2000) Derivatized microfibrillar polysaccharide. WO patent 0047628

Chakraborty A, Sain M, Kortschot M (2006) Reinforcing potential of wood pulp-derived microfibres in a PVA matrix. Holzforschung 60:53–58

Couderc S, Ducloux O, Kim BJ, Someya T (2009) A mechanical switch device made of a polyimide-coated microfibrillated cellulose sheet. J Micromech Microeng 19:055006

Dalmas F, Cavaillé JY, Gauthier C, Chazeau L, Dendievel R (2007) Viscoelastic behaviour and electrical properties of flexible nanofiber filled polymer nanocomposites. Influence of procesing conditions. Comp Sci Technol 67:829–839

De Rodriguez NLG, Thielemans W, Dufresne A (2006) Sisal cellulose whiskers reinforced polyvinyl acetate nanocomposites. Cellulose 13(3):261–270

Dinand E, Chanzy H, Vignon MR, Maureaux A, Vincent I (1996) Microfibrillated cellulose and method for preparing same from primary wall plant pulp, particularly sugar beet pulp. WO patent 9624720

European Standard EN 14257:2006 Adhesives—wood adhesives—determination of tensile strength of lap joints at elevated temperature (WATT'91)

European Standard EN 204:2001 Classification of thermoplastic wood adhesives for non-structural applications

European Standard EN 205:2003 Adhesives—wood adhesives for non-structural applications—determination of tensile shear strength of lap joints

Excoffier G, Vignon M, Benchimol J, Vincent I, Hannuskela T, Chauve V (1999) Parenchyma cellulose substituted with carboxyalkyl groups and preparation method. WO patent 9938892

Eyholzer C, Bordeanu N, Lopez-Suevos F, Rentsch D, Zimmermann T, Oksman K (2009) Preparation and characterization of water-redispersible nanofibrillated cellulose in powder form. Cellulose, under final revision

Eyler RW, Klug ED, Diephuis F (1947) Determination of degree of substitution of sodium carboxymethylcellulose. Anal Chem 19(1):24–27

Goussé C, Chanzy H, Cerrada ML, Fleury E (2004) Surface silylation of cellulose microfibrils: preparation and rheological properties. Polymer 45:1569–1575

Herrick FW (1984) Process for preparing microfibrillated cellulose. US patent 4481077

Hubbe MA, Rojas OJ, Lucia LA, Sain M (2008) Cellulosic nanocomposites: a review. BioRes 3(3):929–980

Hult EL, Larsson PT, Iversen T (2001) Cellulose fibril aggregation—an inherent property of kraft pulps. Polymer 42:3309–3314

Iwamoto S, Nakagaito AN, Yano H (2007) Nano-fibrillation of pulp fibers for the processing of transparent nanocomposites. Appl Phys A: Mater Sci Process 89(2):461–466

Kristo E, Biliaderis CG (2007) Physical properties of starch nanocrystal-reinforced pullulan films. Carbohyd Polym 68:146–158

Kvien K, Oksman K (2007) Orientiation of cellulose nanowhiskers in polyvinyl alcohol. Appl Phys A 87:641–643

Laivins GV, Scallan AM (1993) The mechanism of hornification of wood pulps. In: Baker CF (ed) Products of papermaking. Trans. 10th fundamental research symposium. Pira International, Oxford, pp 1235–1260

Lasseuguette E (2008) Grafting onto microfibrils of native cellulose. Cellulose 15:571–580

Lindström T, Carlsson G (1982) The effect of carboxyl groups and their ionic form during drying on the hornification of cellulose fibers. Svensk Papperstidn 85(15):R146–R151

López-Suevos F, Frazier CE (2005) Parallel-plate rheology of latex films bonded to wood. Holzforschung 59:435–440

López-Suevos F, Frazier CE (2006) The role of resol fortifiers in latex wood adhesives. Holzforschung 60:561–566

Lu J, Wang T, Drzal LT (2008) Preparation and properties of microfibrillated cellulose polyvinyl alcohol composite materials. Compos Part A-Appl S 39(5):738–746

Nakagaito AN, Yano H (2004) The effect of morphological changes from pulp fiber towards nano-scale fibrillated cellulose on the mechanical properties of high-strength plant fiber based composites. Appl Phys A: Mater Sci Process 78(4):547–552

Nakagaito AN, Yano H (2005) Novel high-strength biocomposites based on microfibrillated cellulose having nano-order-unit web-like network structure. Appl Phys A: Mater Sci Process 80(1):155–159

Nakagaito AN, Yano H (2008) The effect of fiber content on the mechanical and thermal expansion properties of biocomposites based on microfibrillated cellulose. Cellulose 15(4):555–559

Roohani M, Habibi Y, Belgacem NM, Ebrahim G, Karimi AN, Dufresne A (2008) Cellulose whiskers reinforced polyvinyl alcohol copolymers nanocomposites. Eur Polym J 44(8):2489–2498

Saito T, Nishiyama Y, Putaux JL, Vignon M, Isogai A (2006) Homogeneous suspensions of individualized microfibrils from TEMPO-catalyzed oxidation of native cellulose. Biomacromolecules 7:1687–1691

Samir M, Alloin F, Paillet M, Dufresne A (2004) Tangling effect in fibrillated cellulose reinforced nanocomposites. Macromolecules 37(11):4313–4316

Sassi JF, Chanzy H (1995) Ultrastructural aspects of the acetylation of cellulose. Cellulose 2:111–127

Stenstad P, Andresen M, Tanem BS, Stenius P (2008) Chemical surface modifications of microfibrillated cellulose. Cellulose 15:35–45

Wågberg L, Decher G, Norgren M, Lindstrom T, Ankerfors M, Axnas K (2008) The build-up of polyelectrolyte multilayers of microfibrillated cellulose and cationic polyelectrolytes. Langmuir 24:784–795

Walecka JA (1956) An investigation of low degree of substitution carboxymethylcelluloses. Tappi 39(7):458–463

Yano H, Nakahara S (2004) Bio-composites produced from plant microfiber bundles with a nanometer unit web-like network. J Mater Sci 39:1635–1638

Yano H, Sugiyama J, Nakagaito AN, Nogi M, Matsuura T, Hikita M, Handa K (2005) Optically transparent composites reinforced with networks of bacterial nanofibers. Adv Mater 17:153–155

Young RA (1994) Comparison of the properties of chemical cellulose pulps. Cellulose 1:107–130

Zadorecki P, Michell AJ (1989) Future-prospects for wood cellulose as reinforcement in organic polymer composites. Polym Compos 10:69–77

Zimmermann T, Pöhler E, Geiger T (2004) Cellulose fibrils for polymer reinforcement. Adv Eng Mat 6(9):754–761

Zimmermann T, Pöhler E, Schwaller P (2005) Mechanical and morphological properties of cellulose fibril reinforced nanocomposites. Adv Eng Mater 7(12):1156–1161